View metadata, citation and similar papers at core.ac.uk

brought to you by CORE

provided by Knowledge Repository of SEMI,CAS

Available online at www.sciencedirect.com

SCIENCE DIRECT

Thin Solid Films 476 (2005) 68–72

thin solid films

www.elsevier.com/locate/tsf

Changing planar thin film growth into self-assembled island formation by adjusting experimental conditions

Jie Sun[a,*], P. Jin[a], Z.G. Wang[a], H.Z. Zhang[b], Z.Y. Wang[b], L.Z. Hu[b]

[a]*Key Laboratory of Semiconductor Materials Science, Institute of Semiconductors, Chinese Academy of Sciences, Beijing 100083, China*
[b]*State Key Laboratory for Materials Modification by Laser, Ion, Electron Beams, Department of Physics, Dalian University of Technology, Dalian 116023, Liaoning Province, China*

Received 5 May 2004; received in revised form 3 September 2004; accepted 7 September 2004
Available online 2 November 2004

Abstract

Illustrated in this paper are two examples of altering planar growth into self-assembled island formation by adapting experimental conditions. Partial oxidation, undersaturated solution and high temperature change Frank–Van der Merwe (FM) growth of $Al_{0.3}Ga_{0.7}As$ in liquid phase epitaxy (LPE) into isolated island deposition. Low growth speed, high temperature and in situ annealing in molecular beam epitaxy (MBE) cause the origination of InAs/GaAs quantum dots (QDs) to happen while the film is still below critical thickness in Stranski–Krastanow (SK) mode. Sample morphologies are characterized by scanning electron microscopy (SEM) or atomic force microscopy (AFM). It is suggested that such achievements are of value not only to fundamental researches but also to spheres of device applications as well.
© 2004 Elsevier B.V. All rights reserved.

PACS: 81.15.Lm; 81.15.Hi
Keywords: Liquid phase epitaxy (LPE); Scanning electron microscopy (SEM); Molecular beam epitaxy (MBE); Atomic force microscopy (AFM)

1. Introduction

The epitaxy modes of thin films can usually be categorized into three types: (a) Frank–Van der Merwe (FM) [1], (b) Stranski–Krastanow (SK) [2] and (c) Volmer–Weber (VW) [3]. These modes are deduced from equilibrium considerations of the surface and interface energies for lattice matched or mismatched systems. The FM mode is simply a layer-by-layer growth, and it usually occurs in lattice well-matched or slightly mismatched systems. In the former case, one may achieve high-quality flat films. In the latter case, films grow excellently until they reach a critical thickness, at which the accumulated elastic strain energy introduces the formation of dislocations. The situation of SK growth, however, is more complicated. In a moderately mismatched system, such as InAs/GaAs, initially, the deposition follows layer-by-layer mechanism which leads to perfect wetting of substrate. Subsequently, when the thickness of pseudomorphic film reaches a certain value d_1, the epitaxial layer is potentially ready to undergo a two-dimensional–three-dimensional (2D–3D) transition. While a further value d_2 (mentioned in literature as "critical thickness") is arrived at, the nucleation and growth of 3D islands will begin, and the system's total energy decreases sharply. Apparently, strain and strain-relaxation by the 3D island formation offer thermodynamic driving force for coherent SK growth. Finally, highly mismatched material combinations, then again, will form islands on the bare unwetted surface, crystallizing in the VW mode.

Modern epitaxial growth techniques, e.g., molecular beam epitaxy (MBE), can fabricate thin films to the atomic dimensional precision. However, in spheres like micro-electromechanical system (MEMS), molecular biology and nanometer micrology, there is also an urgent need to directly control the *lateral* dimension of microstructures and nano-

* Corresponding author. Tel.: +86 10 82304274; fax: +86 10 82305052.
E-mail address: albertjefferson@sohu.com (J. Sun).

0040-6090/$ - see front matter © 2004 Elsevier B.V. All rights reserved.
doi:10.1016/j.tsf.2004.09.016

structures. Hence, selective epitaxy, such as island crystal growth, gradually becomes a focus of attention. Self-organized island growth is particularly attractive, since many requirements for device manufacturing are satisfied, such as less process-induced defects, low cost and easy fabrication, as well as full compatibility with traditional device growth and processing techniques [4]. These self-assembled islands can be accomplished with great skill via SK [5] or VW [6] growth of epilayers, as elucidated above. However, little attention has been concentrated on *changing* planar thin film growth into self-assembled island growth by properly adjusting experimental conditions. In this paper, we show that SK film growth, with the thickness still being less than critical value d_2, and FM layer-by-layer homogeneous epitaxy can both be evolved into self-assembled island formation under certain conditions. Systematic disquisition of altering the epitaxy which ought to have deposited in layer-by-layer manner into self-organized island growth is too complex a topic. In the following discussions, two typical examples are experimentally studied: (a) liquid phase homoepitaxy of $Al_{0.3}Ga_{0.7}As$ islands (FM); (b) molecular beam heteroepitaxy of InAs/GaAs dots (SK).

2. Changing planar growth in FM modus

Generally speaking, during liquid phase epitaxy (LPE) progress on a smooth substrate, the formation of a new monolayer (ML) begins as soon as the monolayer beneath it covers the surface. A flat thin film therefore can be obtained in the FM modus. Nevertheless, in this section, we will focus on micron-sized AlAs–GaAs alloy islands formed by LPE under conditions of partial oxidation, undersaturated solution and high temperature. That research is of great interest from not only a fundamental point of view, but a technological one as well. For instance, in the promising scheme of a certain kind of integrated scanning near-field optical microscopy (SNOM) sensors manufacturing, the fabrication of GaAs microtips plays a very critical part [7]. Although the wet etching process can also yield good quality microtips, it is hard to fulfill monolithic integration of microtips on top of other optical elements because of technological difficulties [7]. Akiyama et al. [8] suggest that one can fabricate microtips on an independent substrate and transfer them onto the target wafer with the tips protected by a resist layer, but that technique seems to be too tedious. In our case, the pyramid-like probe can be conveniently grown onto the facet of the optical element by LPE, thus, there is no problem of the monolithic integration. The reason we choose $Al_{0.3}Ga_{0.7}As$ as test material, however, lies in its easier oxidation and the higher stability of the oxides.

The $Al_{0.3}Ga_{0.7}As$ patterns are created by employing a universal LPE system. The substrate is a 400-μm-thick intrinsic (100) GaAs wafer. After organic abstersion, it is chemically treated in a sulphuric acid cleaning system ($H_2SO_4/H_2O_2/H_2O$=6:1:1). Subsequently, it is washed by deionized water, dried by inert gas, and finally coated with a flat $Al_{0.3}Ga_{0.7}As$ epitaxial layer which serves as a transitive stratum. That newly prepared layer is exposed in extrapure air for 20 min. In order to grow $Al_{0.3}Ga_{0.7}As$ islands, the growth solution should be composed of 500 mg Ga, 25 mg GaAs, 0.6 mg Al and 8.5 mg Ge. In the reducing atmosphere of H_2, a 200-μm-thick layer of growth solution is smeared onto the $Al_{0.3}Ga_{0.7}As$ surface (the temperatures of different samples range from 800 to 810 °C) by a graphite scraper. Afterwards, the wafer temperature is decreased at a rate of 1–1.5 °C min^{-1}. Finally, the $Al_{0.3}Ga_{0.7}As$ hills are turned out when the samples are cooled down to room temperature and scanning electron microscope (SEM) is employed to study their surface conformations.

Under our conditions, 20 min of exposure of the $Al_{0.3}Ga_{0.7}As$ epilayer in the open air results in partial oxidation and many micrometer-sized windows are created due to the chemical property of the oxides. A similar $Al_xGa_{1-x}As$ native oxide matrix is observed by Ghita et al. [9]. Ideal positions for homogeneous nucleation are thus offered by those tiny oxide-free windows. Once stuck onto the windows, clusters of adsorbed particles will act as growth nuclei and grow further by the gathering of migrating particles, becoming large islands consequently by the direction-dependent arrangement of atoms. Nevertheless, the abortion of island growth may occur if the hills are fed by supersaturated sources, for they may overgrow onto the oxides, joint to each other, and finally fuse into a plane. The circumstances of inadequate growth sources should be necessarily produced by maintaining only a skinny layer of undersaturated gallium solution on the $Al_{0.3}Ga_{0.7}As$ surface. It should be pointed out that there is still a small probability for the sources to nucleate on the oxides, generating poor-quality poly-crystalline deposits [10]. Growth at relatively higher temperatures can result in the rapid surface diffusion of materials across the oxides to an opening and favor the desorption of extraneous growth materials from the oxides [11]. Therefore, in our case, high temperature (800–810 °C) has urged self-organized islands

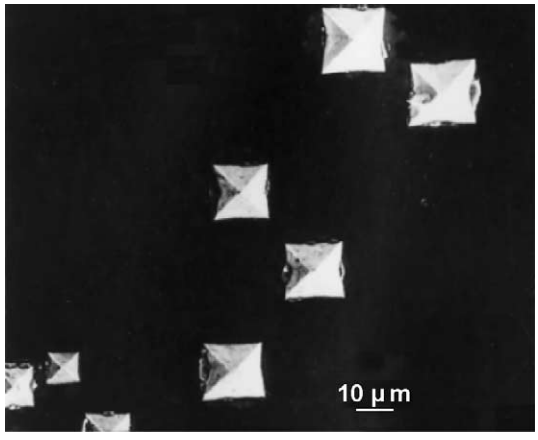

Fig. 1. Several of as-prepared $Al_{0.3}Ga_{0.7}As$ pyramids.

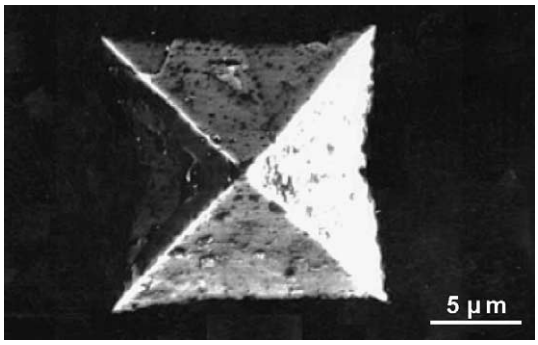

Fig. 2. SEM image of a pyramidal island. The residual of growth solution can be seen.

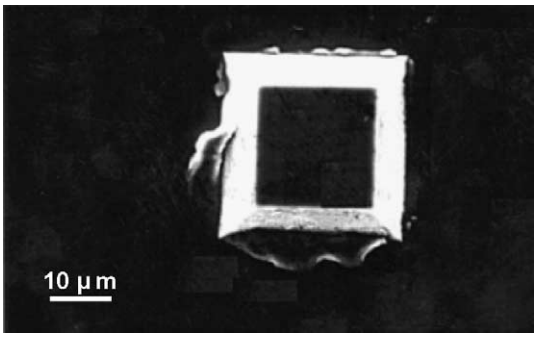

Fig. 4. Enlarged picture of a square-based frustum.

to grow up within the oxide-free windows, and the FM growth is accordingly altered. Summarily, partial oxidation, undersaturated solution and high temperature have led to the formation of $Al_{0.3}Ga_{0.7}As$ islands.

Several as-deposited islands are displayed in Fig. 1, and most of them resemble square-based pyramids. The apex angles on the pyramids' four slopes, directly measured from horizontal view of SEM, are from 70° to 85°, which strongly implies the four slants are not (111)-oriented (that angle of (111) faces should be 60°). The contraction and deformation of the four slope facets are found out in more detail, as can be clearly observed in Fig. 2—a magnified vision of a single pyramid. That is caused by the shape changes of the solution–solid interface during growth, most probably a side effect of Ge doping [12]. A keen zenith of the microtip, which is one of our ultimate goals, is achieved with the curvature radius at the end of the tip being lessened to smaller than 50 nm (geometrically measured by SEM) [13,14]. The authors suggest that the average distance between pyramidal mounds may equal twice the diffusion length of adsorbed particles, just as described in Ref. [15]. Taking this into account, from Fig. 1, we learn that the surface diffusion length is of a considerable magnitude of several tens of microns. That is in agreement with our assumption that high temperature enhances the adatoms' diffusion and helps to create pyramids within the oxide-free windows. For some unknown reasons, none of the islands have developed sharp apexes if we do not add Ge in growth solution, as is shown in Fig. 3. Elongation of growth time is useless in obtaining pointed tops since the sources to grow have already been depleted. In Fig. 3, the gradients of mesas are different, with some at right angles to the bottom surface. Fig. 4 offers a high-magnification microphotograph of a square-based mesa. Though the mechanism of Ge doping is not understood yet, the frustums are believed to be early stages of potential pyramids engendering.

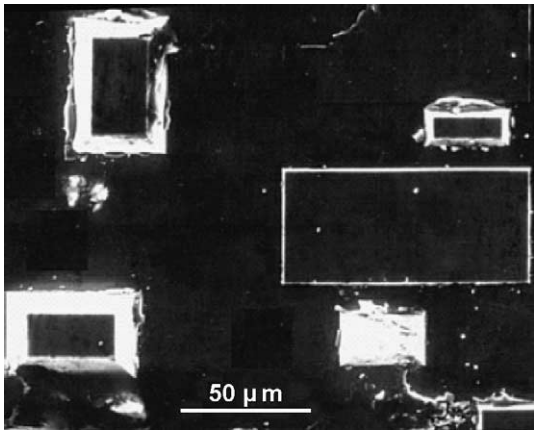

Fig. 3. Various mesas.

3. Changing planar growth in SK modus

We have already changed FM growth in LPE into self-assembled island deposition. In this part, we will concentrate on changing planar growth in SK mode (the initial stage during SK process) into island formation through the enhancement of surface diffusion of deposited materials. We have found that at low deposition rate, high temperature and long growth interruption, extremely low-density quantum dots (QDs) can be achieved while the film thickness is still below the critical thickness d_2. In optical sphere, QDs have to fulfill a set of requirements including a large surface density [16], but, on the contrary, in some electronic applications people tend to attain low-density QDs for facility of quasi-single-QD device fabrication [17]. The density of InAs QDs embedded in InP barriers has been drastically reduced to 4×10^6 cm^{-2} by metal organic vapor phase epitaxy (MOVPE) to make high peak-to-valley ratio resonant tunneling diode [18]. When it comes to InAs/GaAs QDs, the areal density ranges roughly between magnitudes of 10^9 and 10^{11} cm^{-2} [19,20]. Thereinafter, by means of changing SK growth mode, we manage to reduce the InAs/GaAs QD density to as small as 2.48×10^7 cm^{-2}, which is low enough to meet the needs of certain electronic applications.

The samples are prepared in MBE system under an As_2 flux of 5×10^{-6} torr beam equivalent pressure. On the semi-insulating (100) GaAs wafer, 100 nm undoped GaAs buffer layer is grown at a substrate temperature T_s of 580 °C. Then, T_s is lowered to 500 °C and another 2 nm GaAs barrier is

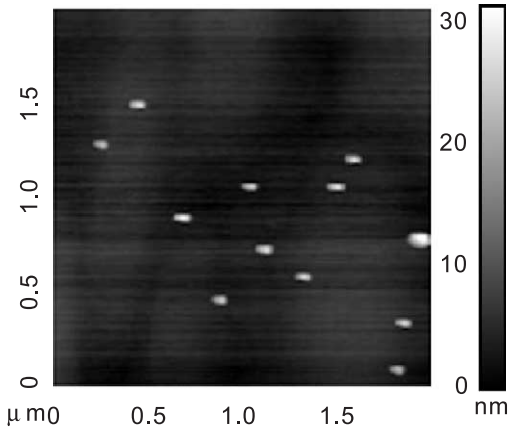

Fig. 5. AFM image of low-density InAs QDs realized on (100) GaAs at 500 °C after 2 min of annealing.

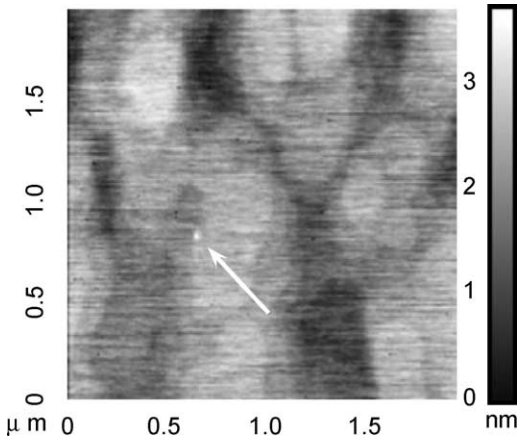

Fig. 7. Low-density QDs of 2.48×10^{7} cm^{-2}. The QD is indicated by arrows.

deposited. Afterwards, with an exceedingly slow rate of 0.008 ML/s, nominally 1.52 ML InAs, as is slightly less than d_2, are deposited. (By growing a reference sample, we learn that the critical thickness d_2 for InAs quantum dot origination on 500 °C—(100) GaAs under our experimental conditions lies at ~1.6 ML.) Finally, the deposited InAs undergoes 2 min of growth interruption (namely in situ annealing) at 500 °C. As-grown InAs is not capped by GaAs, and the surface profile is detected by ex situ atomic force microscope (AFM).

Fig. 5 shows InAs QDs of 4.10×10^{8} cm^{-2} prepared in the above-mentioned manner. The low-density quantum dots are well isolated, 13 nm high and 69 nm wide on an average. During SK growth, theoretically, when deposited InAs thickness reaches d_1, it leaves the *stable* 2D wetting of the substrate and enters into a *metastable* 2D growth area in which a supercritically thick wetting layer builds up (pp. 430 in Ref. [21]). No 3D nucleation will come about unless a larger thickness value d_2 is arrived at. However, since the 2D growth, with InAs thickness standing between d_1 and d_2, is of a metastable state, one could still change the epitaxy in this phase into 3D island formation by appropriately adjusting the conditions. Calculations based on energetic considerations have shown that a 2D island will transform into a pyramidal 3D island whenever it exceeds a certain limiting size [22,23]. This is the kinetic pathway by which 2D patterns evolve into QDs. Hence, at the same deposition amount, it is reasonable to expect an individual 2D island to reach the limiting size more easily if surface diffusion of deposited InAs (or simply In) is improved. That is, InAs gather at 2D nuclei more effectively, and the 2D islands are larger and of lower density. That makes it possible to fabricate low-density QDs under critical thickness d_2. Through Monte Carlo simulation, Ghaisas et al. [24] find out that diffusion length increases with a decrease in growth speed, and can be expressed as an exponential function. Furthermore, it is known that the migration of deposited InAs can be enhanced during dot growth interruption [25], for the wafer is maintained at high temperature. Therefore, in our experiment, low deposition rate, high growth temperature and long-time in situ annealing all result in a promoted surface diffusion effect. The layer-by-layer growth of SK mode is consequently altered into self-organized island deposition.

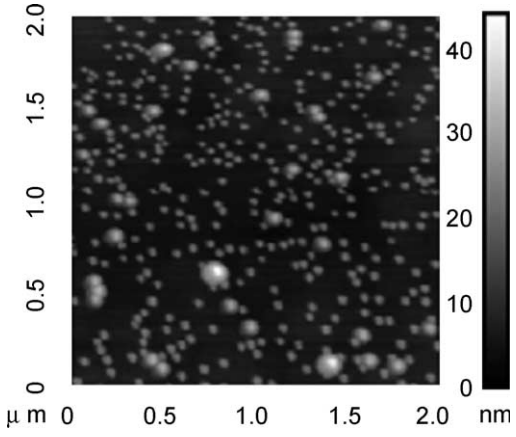

Fig. 6. Surface morphology of the non-homogeneous sample where InAs coverage is the thickest.

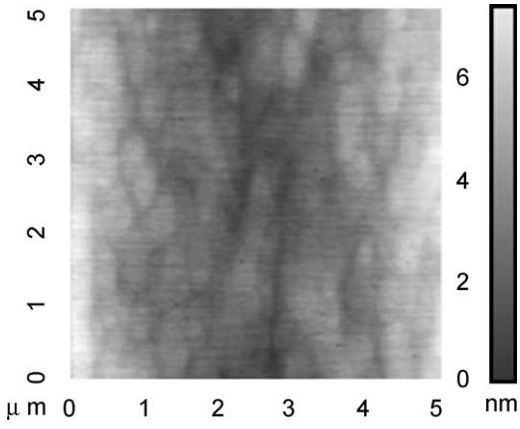

Fig. 8. AFM image of the inhomogeneous sample where InAs coverage is the thinnest. There are no QDs and only 2D islands exist.

According to the mechanism discussed above, it seems that a further reduction of InAs deposition might result in an even lower QD density. However, too small an InAs depositional amount (below d_1) will not fill the needs of evolving 2D patterns into QDs. Because d_1 and d_2 are exceedingly close to each other (pp. 442 in Ref. [21]), it is difficult to precisely control these thicknesses via MBE. Thus, in order to explore the low extremity of QD density of this fabrication method, we intentionally grow a highly inhomogeneous sample where the InAs coverage varies continuously along the surface. The 2-in. sample is prepared in the same way as elucidated above except that wafer rotation is stopped during InAs growth. The wafer is located at the center of the 3-in. Mo-block. Different parts on the sample have different InAs coverages, which are due to different distances apart from the In effusion cell. Basically, we find nanodot density and size (both height and width) increase with InAs deposition amount. Fig. 6 shows surface morphology of the sample where InAs coverage is the biggest. The QDs are 8~16 nm high and 57~88 nm wide, and have a density of 1.21×10^{10} cm^{-2}. Situation of the smallest InAs QD density of 2.48×10^{7} cm^{-2} is exhibited in Fig. 7. The QDs are 2–3 nm in height and 46–88 nm in width. In Fig. 8, where the InAs amount reaches its smallest value, we get no QDs but 2D patterns. On the whole, QDs grown in our experiment are bigger than conventional InAs/GaAs QDs [26], implying the large 2D islands caused by strengthened surface diffusion during the beginning stage of QD evolvement. (The enlarged 2D islands can also be seen in Fig. 8 clearly).

4. Conclusion

To sum up, we have successfully changed planar thin film growth into self-assembled island formation by properly adjusting experimental conditions. Two typical tests have been shown: (a) pyramidal $Al_{0.3}Ga_{0.7}As$ islands grown by LPE (FM); (b) extremely low-density InAs/GaAs QDs grown by MBE (SK). That accomplishment would contribute not only to crystal growth theory, but also to miniature manufacturing technology. This notwithstanding, some conundrums still cannot be illustrated refinedly and further endeavor is needed. The use of SiO_2 mask with lithographed windows may be beneficial in controlling the sizes and location of $Al_{0.3}Ga_{0.7}As$ islands. Device structures should be fabricated to verify the electrical properties of low-density QDs. Those are both our future research goals.

Acknowledgements

The authors gratefully acknowledge the financial support from “Special Funds for Major State Basic Research Project of China (Nos. G2000068303 and 2002CB311905)” and “National Natural Science Foundation of China (No. 60377005)”. Part of this work is accomplished with the help from Ms. C.L. Yan.

References

[1] F.C. Frank, J.H. Van der Merwe, Proc. R. Soc. Lond., Ser. A 198 (1949) 205.
[2] I.N. Stranski, L. Krastanow, Sitz.Ber.-Akad. Wiss. Math.-Nat.wiss. Kl. Abt. IIb 146 (1938) 797.
[3] M. Volmer, A. Weber, Z. Phys. Chem. 119 (1926) 277.
[4] Z.G. Wang, Y.H. Chen, F.Q. Liu, B. Xu, J. Cryst. Growth 227–228 (2001) 1132.
[5] Z.G. Wang, J. Wu, Microelectron. J. 34 (2003) 379.
[6] T. Godfroid, R. Gouttebaron, J.P. Dauchot, Ph. Leclere, R. Lazzaroni, M. Hecq, Thin Solid Films 437 (2003) 57.
[7] C. Gorecki, S. Khalfallah, H. Kawakatsu, Y. Arakawa, Sens. Actuators, A, Phys. 87 (2001) 113.
[8] T. Akiyama, U. Staufer, N.F. de Rooij, IEEE J. Microelectromechanical Syst. 8 (1999) 65.
[9] R.V. Ghita, E. Vasile, D. Cengher, Thin Solid Films 338 (1999) 46.
[10] T.F. Kuech, J. Cryst. Growth 115 (1991) 52.
[11] H. Heinecke, A. Brauers, F. Grafahrend, C. Plass, N. Pütz, K. Werner, M. Weyers, H. Lüth, J. Cryst. Growth 77 (1986) 303.
[12] P.G. Barber, R.F. Berry, W.J. Debnam, A.L. Fripp, G. Woodell, R.T. Simchick, J. Cryst. Growth 147 (1995) 83.
[13] L.Z. Hu, J. Sun, Q.D. Meng, Y.M. Su, Y. Zhao, J. Cryst. Growth 240 (2002) 98.
[14] Y.M. Su, L.Z. Hu, J. Sun, Q.D. Meng, Y. Zhao, Z.Y. Wang, Proc. SPIE 4923 (2002) 41.
[15] M. Shimbo, J. Nishizawa, T. Terasaki, J. Cryst. Growth 23 (1974) 267.
[16] M.J. da Silva, A.A. Quivy, P.P. Gonzalez-Borrero, E. Marega Jr., J. Cryst. Growth 236 (2002) 41.
[17] T. Bryllert, M. Borgstrom, L.-E. Wernersson, W. Seifert, L. Samuelson, Appl. Phys. Lett. 82 (2003) 2655.
[18] M. Borgstrom, T. Bryllert, T. Sass, B. Gustafson, L.-E. Wernersson, W. Seifert, L. Samuelson, Appl. Phys. Lett. 78 (2001) 3232.
[19] S. Muto, Y. Ebiko, D. Suzuki, S. Itoh, K. Shiramine, T. Haga, Y. Nakata, Y. Sugiyama, N. Yokoyama, Mater. Sci. Semicond. Process. 1 (1998) 131.
[20] Z.G. Wang, F.Q. Liu, J.B. Liang, B. Xu, Sci. China, Ser. A Math. Phys. Astron. Technol. Sci. 43 (2000) 861.
[21] W. Seifert, N. Carlsson, M. Miller, M.-E. Pistol, L. Samuelson, L.R. Wallenberg, Prog. Cryst. Growth Charact. 33 (1996) 423.
[22] C. Priester, M. Lannoo, Phys. Rev. Lett. 75 (1995) 93.
[23] Y. Chen, J. Washburn, Phys. Rev. Lett. 77 (1996) 4046.
[24] S.V. Ghaisas, S. Das. Sarma, Phys. Rev., B 46 (1992) 7308.
[25] G.E. Cirlin, G.M. Guryanov, A.O. Golubok, S. Ya. Tipissev, N.N. Ledentsov, P.S. Kop’ev, M. Grundmann, D. Bimberg, Appl. Phys. Lett. 67 (1995) 97.
[26] Q. Xie, P. Chen, A. Madhukar, Appl. Phys. Lett. 65 (1994) 2051.